Quantum Hall Effect in Thin Films of Three-Dimensional Topological Insulators

Huichao Li[1], L. Sheng[1],* and D. Y. Xing[1]†
[1] National Laboratory of Solid State Microstructures and Department of Physics, Nanjing University, Nanjing 210093, China

We show that a thin film of a three-dimensional topological insulator (3DTI) with an exchange field is a realization of the famous Haldane model for quantum Hall effect (QHE) without Landau levels. The exchange field plays the role of staggered fluxes on the honeycomb lattice, and the hybridization gap of the surface states is equivalent to alternating on-site energies on the AB sublattices. A peculiar phase diagram for the QHE is predicted in 3DTI thin films under an applied magnetic field, which is quite different from that either in traditional QHE systems or in graphene.

PACS numbers: 73.43.-f,71.70.Ej,75.70.Tj,72.10.Bg

Introduction.–Haldane was the first to realize that quantum Hall effect (QHE) can happen in systems without Landau levels (LLs). He proposed a spinless electron model [1] defined on a two-dimensional (2D) honeycomb lattice with staggered magnetic fluxes and alternating on-site energies on the AB sublattices. In the model, the electrons retain their usual Bloch state character, but exhibit a nonzero quantized Hall conductivity σ_{xy} by simulation of the "parity anomaly" of $(2+1)$D field theories, now termed as quantum anomalous Hall effect. The Haldane model breaks time-reversal symmetry. Kane and Mele [2] suggested that the single-atomic-layer graphene with intrinsic spin-orbit coupling constitutes two copies of the Haldane model. Since the two spin components are mutually conjugate under time reversal, the Kane-Mele model restores the time reversal symmetry. While the two spin components contribute oppositely to the charge Hall conductivity, the model displays a novel quantum spin Hall effect (QSHE). The QSHE has been experimentally observed in quantum wells of mercury telluride [3], instead of graphene. A great deal of research interest in the QSHE in recent years has led to the birth of topological insulators, which include a class of 2D and 3D band insulators with nontrivial band topology [4].

A 3D topological insulator [5, 6] (3DTI) is featured with the presence of conducting surface states in the bulk band gap, which are topologically protected and insensitive to impurity scattering. On an isolated surface of the 3DTI, the energy spectrum of the surface states constitutes a single massless spin-momentum-locked Dirac cone [7], which offers a unique platform to realize some exotic relativistic quantum phenomena, such as Majorana fermions [8]. In a perpendicular magnetic field B_0, the surface states are quantized into LLs with energies $E_n = \mathrm{sgn}(n)\sqrt{2eB_0 v_F^2|n|}$ (in $\hbar = c = 1$ units), where $n = 0, \pm1, \pm2\cdots$ and v_F is the Fermi velocity. Due to the existence of the zero-mode ($n = 0$) LL, which is particle-hole symmetric, the Hall conductivity is expected to be half-integer quantized [6] $\sigma_{xy} = \nu\frac{e^2}{h}$, where $\nu = \ell + \frac{1}{2}$ with ℓ being an integer. Exciting experimental progress has been made recently. Cheng *et al*. and Hanaguri *et al*. [9] detected the surface states in Bi_2Se_3 to form LLs in the presence of an applied magnetic field. Very recently, Brüne *et al*. [10] carried out a Hall conductivity measurement in a high-quality strained HgTe layer, and observed a sequence of Dirac-like Hall plateaus, which was ascribed to the topological surface states. It was also suggested theoretically that electrons in the surface states of a 3DTI with exchange splitting could give rise to a QHE in the absence of an applied magnetic field, i.e., the quantum anomalous Hall effect [11]. For a thin film of a 3DTI, the finite-size confinement will mix the surface states at the top and bottom surfaces and create a hybridization energy gap in the spectrum of the surface states [12, 13]. The hybridization gap can be controlled by tuning the thickness of the 3DTI film [12, 13]. The exchange field (or equivalently a Zeeman energy) and the hybridization gap effectively add different types of mass to the Dirac fermions [14] and provide ways to control the properties of the surface states, but their effect on the QHE has not been well understood.

The Haldane's QHE model [1] has been difficult to be realized in condensed matter systems, though Shao *et al*. [15] suggested recently that it could be simulated by using ultracold atoms. In this Letter, we propose that a thin film of a 3DTI in the presence of an exchange field is a natural realization of the Haldane model. The exchange field plays the role of the staggered fluxes in the Haldane model, and the hybridization gap is equivalent to the alternating on-site energies on AB sublattices. Under an applied magnetic field, a 3DTI thin film and the Haldane model are still equivalent in Hamiltonian form, so that we can study the QHE in the 3DTI film conveniently based upon the Haldane model. The other purpose of this Letter is to report a peculiar phase diagram for the QHE in thin films of 3DTIs, due to the interplay between Zeeman energy g and hybridization gap Δ. For $\Delta = 0$, a nonzero g only shifts the positions of the LLs without creating new Hall plateaus. If $g = 0$ but $\Delta \neq 0$, a new $\nu = 0$ plateau will appear, in addition to the original $\nu = 2(\ell+\frac{1}{2})$ odd-integer plateaus. The simultaneous presence of nonzero g and Δ causes splitting of the odd-integer

Hall plateaus, and so all integer ($\nu = \ell$) plateaus emerge. More interestingly, as the product of g and Δ is equal to certain critical values, the split plateaus can merge again, and most odd-integer (or even-integer) plateaus disappear.

Thin Films of 3DTIs.–We start with an effective Hamiltonian for electrons in the surface states of a 3DTI thin film [13] with an exchange energy [11]

$$H(k) = -Dk^2 + v_F(k_y\hat{\sigma}_x - k_x\hat{\sigma}_y) + (\frac{\Delta}{2} - Bk^2)\tau_z\hat{\sigma}_z + g\hat{\sigma}_z . \quad (1)$$

Here, the first two terms are the Hamiltonian for two isolate surfaces with v_F the Fermi velocity, $\mathbf{k}$ is the momentum with respect to Dirac point Γ, and $\hat{\sigma}_\alpha$ are the Pauli matrices for electron spin with $\alpha = x, y, z$. The third term stands for the coupling between the upper and lower surface states of the thin film with $\tau_z = 1$ (-1) representing the bonding (antibonding) between them, and the last one is the exchange field with strength g. We will consider the case, where the condition $B^2 - D^2 > 0$ for band inversion is satisfied [13]. Since Hamiltonian (1) is block diagonal for $\tau_z = \pm 1$, the Chern numbers C_{τ_z} of the occupied valence bands with $\tau_z = +1$ and -1 can be calculated separately, yielding $C_{\tau_z} = -\tau_z[\mathrm{sgn}(B) + \mathrm{sgn}(\Delta + 2g\tau_z)]/2$. The total Chern number $C = C_+ + C_-$ is given by

$$C = \frac{1}{2}[\mathrm{sgn}(\Delta - 2g) - \mathrm{sgn}(\Delta + 2g)] . \quad (2)$$

We note that even though the τ_z-dependent Chern numbers depend on the sign of parameter B, the total Chern number is independent of B. In Fig. 1, we show the phase diagram of the 3DTI thin film in the presence of exchange splitting. Lines $g = -\Delta/2$ and $g = -\Delta/2$ are the critical boundaries between the normal insulator with $C = 0$ and the Chern insulator with $C = \pm 1$, the latter being in the lower and upper shaded regions. In the regions of $C = \pm 1$, quantum anomalous Hall effect with $\sigma_{xy} = \pm\frac{e^2}{h}$ occurs.

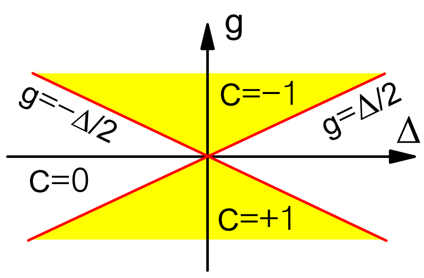

FIG. 1: Schematic phase diagram on the hybridization potential Δ and exchange energy g plane, in which two solid lines $g = \pm\Delta/2$ separate four phase regions with $C = \pm 1$ and $C = 0$.

Haldane Model.–The Hamiltonian of the Haldane model reads [1]

$$H = -\sum_{\langle i,j\rangle} t c_i^\dagger c_j + \sum_{\langle\langle i,j\rangle\rangle} t_2 e^{i\phi_{ij}} c_i^\dagger c_j + \sum_i V_i c_i^\dagger c_i . \quad (3)$$

Here, $c_i^\dagger$ (c_i) is the fermion creation (annihilation) operator at site i, t (t_2) is the hopping integral between the nearest-neighbor (next-nearest-neighbor) sites i and j, and $V_i = \pm M$ for sublattices A and B, respectively. $\phi_{ij} = \pm\phi$ is the accumulated Peierls phase from site i to its second neighbor j, due to a staggered magnetic-flux density, where the positive sign is taken for an electron hopping along the arrows indicated in the Fig. 1 of Ref. [1]. It has been shown [1] that the Haldane model (3) exhibits a quantized Hall conductivity $\pm\frac{e^2}{h}$ for $3\sqrt{3}|t_2 \sin\phi| > |M|$, and behaves as a normal insulator otherwise.

The low-energy behavior of electrons in the Haldane model is governed by the dispersion relation near the two inequivalent Dirac points K and K'. We can expand the Hamiltonian to the linear order in the relative momentum $\mathbf{k}$ with respect to the two Dirac points, and obtain

$$H(k) = v_F(\tau_z k_y\hat{\sigma}_x - k_x\hat{\sigma}_y) + \frac{\Delta}{2}\hat{\sigma}_z + g\tau_z\hat{\sigma}_z . \quad (4)$$

Here, $v_F = 3at/2$, $\Delta/2 = M$, $g = -3\sqrt{3}t_2\sin\phi$, and a constant energy $-3t_2\cos\phi$ has been omitted. $\hat{\sigma}_\alpha$ represent two sublattices and $\tau_z = \pm 1$ correspond to two Dirac valleys. Using a unitary transformation $H' = U^\dagger H U$ in Eq. (4) with $U = [1 + \hat{\sigma}_y + (1 - \hat{\sigma}_y)\tau_z]/2$, we obtain $H'(k) = v_F(k_y\hat{\sigma}_x - k_x\hat{\sigma}_y) + \frac{\Delta}{2}\tau_z\hat{\sigma}_z + g\hat{\sigma}_z$. To the linear order of k, $H'(k)$ is identical in form to Eq. (1), even though parameters in the two Hamiltonians have different physical meanings. More importantly, the condition for the occurrence of the quantum anomalous Hall effect in the Haldane model [1], $3\sqrt{3}|t_2\sin\phi| > |M|$, is also identical to that for a 3DTI thin film, i.e., $|g| > |\Delta|/2$ as shown in Fig. 1, due to the mapping of parameters below Eq. (4). Therefore, a 3DTI thin film in the presence of an exchange energy is a natural realization of the Haldane model. The exchange energy plays the role of the staggered fluxes in the Haldane model, and the hybridization gap of the surface states is equivalent to the alternating on-site energies.

Quantum Hall Effect of 3DTI Thin Films.–We now study the QHE in a thin film of a nonmagnetic 3DTI. As a perpendicular magnetic field B_0 is applied to the film, the action on the spin degrees of freedom is the Zeeman energy, which can be described by the last term, $g\sigma_z$ in Eq. (1) (with $g = g_{eff}\mu_B B_0$); and the action on the orbital motion can be included by use of the Peierls substitution $\mathbf{k} \to (\mathbf{k} - e\mathbf{A})$ with $\mathbf{A}$ the vector potential due to B_0. Since the unitary transformation U introduced above does not affect the orbital degrees of freedom, it is apparent that Hamiltonian (1) is still equivalent to the

Haldane model given by Eqs. (3) and (4) in this case, provided that the same vector potential $\mathbf{A}$ is included into these equations. As a result, the QHE in a thin film of a 3DTI is equivalent to that in the Haldane model. The LLs in the Haldane model Eq. (4) subject to a magnetic field have been solved in the original work of Haldane [1]

$$E_{\tau_z,n} = \mathrm{sgn}(n)\sqrt{w_1^2|n| + \left(\frac{\Delta}{2} + g\tau_z\right)^2}, \quad (5)$$

for nonzero integer n, and

$$E_{\tau_z,0} = [g + (\Delta/2)\tau_z]\mathrm{sgn}(eB_0)\ , \quad (6)$$

for $n = 0$. Here, $w_1 = \sqrt{2|eB_0|}v_F$ is the width of the $\nu = 1$ Hall plateau at $g = \Delta = 0$. When both g and Δ vanish, Eqs. (5) and (6) reduce to the standard LLs for massless Dirac fermions, which are additionally degenerate for $\tau_z = \pm 1$, i.e., $E_{+,n} = E_{-,n}$. Nonzero g and Δ may shift the relative positions of the LLs and cause the LLs to split, which will determine the quantization rule of the Hall conductivity.

The Hall conductivity will be calculated numerically from Eq. (3) by setting $\phi = \pi/2$ in a system of size 64×64. The vector potential of the applied magnetic field is introduced into Eq. (3) via the integral form of the Peierls substitution $t \to te^{i\theta_{ij}}$ ($t_2 \to t_2 e^{i\theta_{ij}}$), where $\theta_{ij} = e\int_i^j \mathbf{A}\cdot d\boldsymbol{l}$ with the integral being along the electron hopping path. The magnetic flux per hexagon is given by $\varphi = \sum_{ij}\theta_{ij} = \pi B_0 3\sqrt{3}a^2/\phi_0 = 2\pi/M_0$, where the summation runs over six links around a hexagon, $\phi_0 = h/e$ is the flux quantum, and M_0 is an integer. The Hall conductivity at zero temperature can be calculated by use of the standard Kubo formula

$$\sigma_{xy} = \frac{4e^2}{S}\sum_{\varepsilon_m < E_F < \varepsilon_n} \frac{\mathrm{Im}(\langle n|v_x|m\rangle\langle m|v_y|n\rangle)}{(\varepsilon_m - \varepsilon_n)^2}\ . \quad (7)$$

Here, ε_m and ε_n are the eigenenergies corresponding to occupied state $|m\rangle$ and empty state $|n\rangle$, respectively. S is the area of the hexagon lattice, and v_α is the velocity operator with $\alpha = x$ or y. With tuning chemical potential E_F, a series of integer-quantized plateaus of σ_{xy} will appear, each one corresponding to E_F moving in the gaps between two neighboring LLs. When $g = \Delta = 0$, Eq. (3) reduces to the tight-binding model for graphene without spin degrees of freedom. It follows that the Hall conductivity in the 3DTI thin film is half of that in graphene. The Hall conductivity for the 3DTI thin film is thus odd-integer quantized $\sigma_{xy} = 2(\ell + \frac{1}{2})\frac{e^2}{h}$ with the prefactor 2 originating from two surfaces, as expected.

In Fig. 2, the calculated Hall conductivity σ_{xy} in units of $\frac{e^2}{h}$ is plotted as a function of E_F/w_1 with magnetic flux $\varphi = 2\pi/1024$ for some different values of g and Δ. From Eqs. (5) and (6), we can see that for $g \neq 0$ and $\Delta = 0$, while their positions shift with g, all the LLs are still degenerate for $\tau_z = \pm 1$, so that the total Hall conductivity remains to be odd-integer quantized $\sigma_{xy} = (2\ell + 1)\frac{e^2}{h}$, as shown in Fig. 2(a). For $g = 0$ and $\Delta \neq 0$, the LLs with $n \neq 0$ are degenerate for $\tau_z = \pm 1$, but there is a splitting of the $n = 0$ LL, yielding a new plateau of $\sigma_{xy} = 0$, as shown in Fig. 2(b). For $g \neq 0$ and $\Delta \neq 0$, the additional degeneracy of all the LLs is generally lifted,

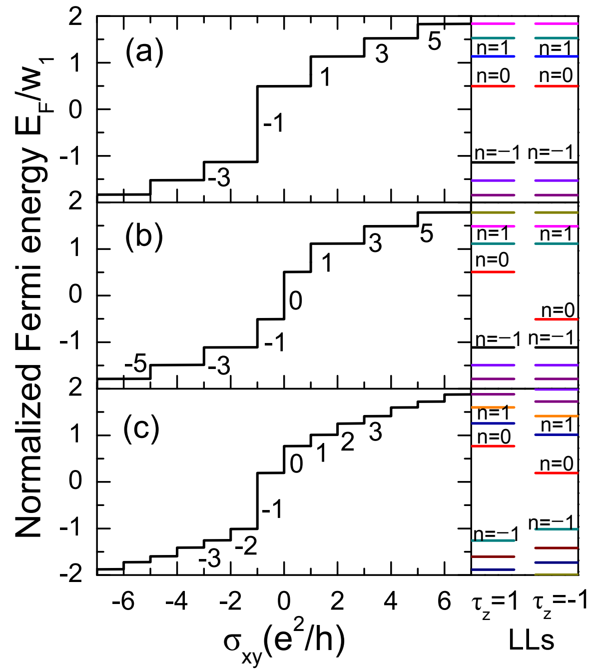

FIG. 2: Calculated Hall conductivity σ_{xy} in units of e^2/h as a function of E_F with magnetic flux $\varphi = 2\pi/1024$ for (a) $g = 0.5w_1$ and $\Delta = 0$, (b) $g = 0$ and $\Delta = w_1$, and (c) $g = 0.5w_1$ and $\Delta = 0.6w_1$. The corresponding LL energies for $\tau_z = \pm 1$ are shown in the right panel.

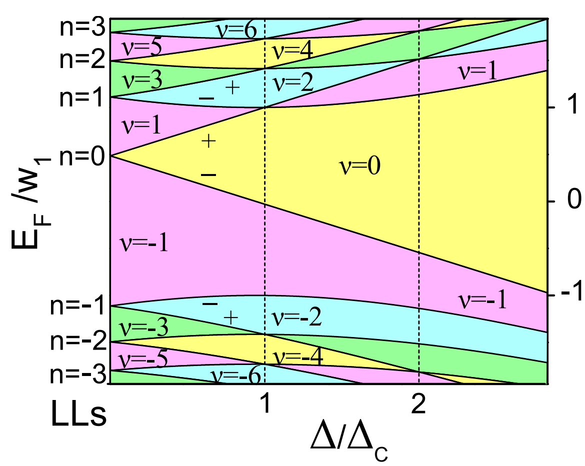

FIG. 3: Phase diagram for the QHE on the E_F/w_1 versus Δ/Δ_c plane. The phase boundary is determined by the energies of the LLs as functions of Δ/Δ_c, calculated from Eqs. (5) and (6). Here, $\Delta_c = w_1^2/2g$, and the Zeeman energy is taken to be $g = 0.5w_1$.

and each degenerate LL splits apart into two so that all integer Hall plateaus $\sigma_{xy} = \ell\frac{e^2}{h}$ appear, as shown in Fig. 2(c).

In Fig. 3, we plot the energies of the LLs calculated from Eqs. (5) and (6) as functions of Δ for a fixed Zeeman energy, which effectively determine a phase diagram for the QHE on the E_F versus Δ plane. The splitting of each LL increases with Δ, which can be understood from Eqs. (5) and (6). Interestingly, when Δ is integer multiples of certain critical value Δ_c, the LLs for $\tau_z = \pm 1$ and different n cross each other at the same time, leading to disappearance of nearly half of the Hall plateaus. For example, $E_{+,n} = E_{-,n+1}$ at $\Delta = \Delta_c$, $E_{+,n} = E_{-,n+2}$ at $\Delta = 2\Delta_c$, and on analogy of this, for $n \geq 0$. The LLs for $n < 0$ cross in a similar manner. It is straightforward from Eq. (5) to obtain $g\Delta_c = w_1^2/2$ or $\Delta_c = w_1^2/2g$. The Hall conductivity as a function of E_F is shown in Fig. 4(a) at $\Delta = \Delta_c$ and 4(b) at $\Delta = 2\Delta_c$, respectively. In the former, the Hall conductivity $\sigma_{xy} = \nu\frac{e^2}{h}$ is quantized into even-integer $\nu = 2\ell$ plateaus plus a single odd-integer $\nu = -1$ plateau, and in the latter, it displays odd-integer $\nu = (2\ell+1)$ plateaus plus two even-integer 0 and -2 plateaus. In both cases, the split Hall plateaus merge again partly, and most odd-integer [even-integer] plateaus disappear in Fig. 4(a) [4(b)].

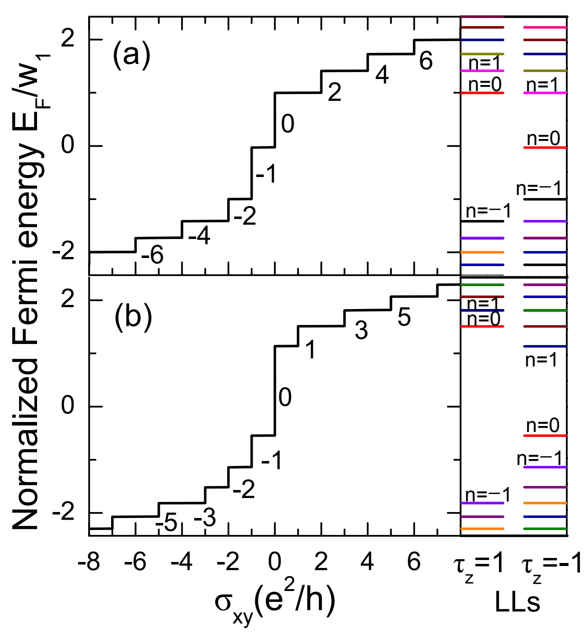

FIG. 4: Calculated Hall conductivity σ_{xy} in units of e^2/h as a function of E_F with magnetic flux $\varphi = 2\pi/1024$ for (a) $g = 0.5w_1$ and $\Delta = w_1$, and (b) $g = 0.5w_1$ and $\Delta = 2w_1$. The corresponding LL energies for $\tau_z = \pm 1$ are shown in the right panel.

Summary.– In summary, we have shown that the Haldane model for the QHE without LLs can be realized in condensed matter systems by use of a 3DTI thin film with an exchange field. As a perpendicular magnetic field is applied to the 3DTI thin film, Hamiltonian (1) and Eq. (4) for the Haldane model are still equivalent to each other, provided that the vector potential **A** is included in both equations. A rich phase diagram for the QHE in the 3DTI thin film is predicted as a consequence of the interplay between g and Δ. The simultaneous presence of nonzero g and Δ causes splitting of original odd-integer Hall plateaus $\sigma_{xy} = (2\ell+1)\frac{e^2}{h}$ into $\sigma_{xy} = \ell\frac{e^2}{h}$. Remarkably, when the product of g and Δ is at certain critical values, the plateaus can merge again partly, and most odd-integer (or even-integer) plateaus disappear.

Acknowledgments.–This work is supported by the State Key Program for Basic Researches of China under Grant Nos. 2009CB929504, 2007CB925104 (LS), 2011CB922103 and 2010CB923400 (DYX), the National Natural Science Foundation of China under Grant Nos. 10874066 and 11074110, and the Science Foundation of Jiangsu Province in China under Grant No. SBK200920627.

* Electronic address: shengli@nju.edu.cn
† Electronic address: dyxing@nju.edu.cn

[1] F.D.M. Haldane, Phys. Rev. Lett. 61, 2015 (1988).
[2] C.L. Kane and E.J. Mele, Phys. Rev. Lett. **95**, 226801 (2005).
[3] B.A. Bernevig, T.L. Hughes, and S.C. Zhang, Science **314**, 1757 (2006); M. Koñig, S. Wiedmann, C. Brune, A. Roth, H. Buhmann, L.W. Molenkamp, X.L. Qi, and S.C. Zhang, Science **318**, 766 (2007).
[4] M. Z. Hasan and C. L. Kane, Rev. Mod. Phys. **82**, 3045 (2010); X. L. Qi and S. C. Zhang, Rev. Mod. Phys., (in the press, cond-mat/10122330).
[5] J. E. Moore and L. Balents, Phys. Rev. B 75, 121306 (2007).
[6] L. Fu, C. L. Kane, and E. J. Mele, Phys. Rev. Lett. 98, 106803 (2007); L. Fu and C. L. Kane, Phys. Rev. B 76, 045302 (2007).
[7] D. Hsieh, *et al.*, Nature **452**, 970 (2008); Y. Xia, *et al.*, Nature Physics **5**, 398 (2009); D. Hsieh, *et al.*, Science **323**, 919 (2009); D. Hsieh, *et al.*, Nature **460**, 1101 (2009).
[8] L. Fu and C. L. Kane, Phys. Rev. Lett. **100**, 096407 (2008).
[9] P. Cheng, *et al.*, Phys. Rev. Lett. **105**, 076801 (2010); T. Hanaguri, K. Igarashi, M. Kawamura,H. Takagi, and T. Sasagawa, Phys. Rev. B 82, 081305(2010).
[10] C. Brüne *et al.*, Phys. Rev. Lett. **106**, 126803 (2011).
[11] X.-L. Qi, Y.-S. Wu, and S.-C. Zhang, Phys. Rev. B 74, 085308 (2006); C.-X. Liu, X.-L. Qi, X. Dai, Z. Fang, and S.-C. Zhang, Phys. Rev. Lett. 101, 146802 (2008); H. Zhang, C. Liu, X. Qi, X. Dai, Z. Fang, and S. Zhang, Nature Physics 5, 438 (2009); R. Yu, W. Zhang, H.-J. Zhang, S.-C. Zhang, X. Dai, and Z. Fang, Science 329, 61 (2010).
[12] J. Linder, T. Yokoyama, and A. Sudbø, Phys. Rev. B 80, 205401 (2009); Liu, C-X. *et al.* **81**, 041307(R) (2010);
[13] W.-Y. Shan, H.-Z. Lu, S.-Q. Shen, New J. Phys. 12,043048 (2010); H.-Z. Lu, W.-Y. Shan, W. Yao, Q.

Niu, and S.-Q. Shen, Phys. Rev. B 81, 115407 (2010); H. Li, L. Sheng, D. N. Sheng, and D. Y. Xing Phys. Rev. B 82, 165104 (2010).

[14] S. Q. Shen, cond-mat/09094125 (2009).

[15] L. B. Shao, Shi-Liang Zhu, L. Sheng, D. Y. Xing, and Z. D. Wang, Phys. Rev. Lett. **101**, 246810 (2008)